BBA - Molecular Basis of Disease 1865 (2019) 1126–1137

Contents lists available at ScienceDirect

BBA - Molecular Basis of Disease

journal homepage: www.elsevier.com/locate/bbadis

# Hypothalamic expression of the atypical chemokine receptor ACKR2 is involved in the systemic regulation of glucose tolerance☆

Milena Fioravante[a,b], Bruna Bombassaro[a,b], Albina F. Ramalho[a,b], Rodrigo F. de Moura[a,b], Roberta Haddad-Tovolli[a,b], Carina Solon[a,b], Nathalia R. Dragano[a,b], Jean F. Vettorazzi[b,c], Rodrigo S. Gaspar[b,d], Eduardo R. Ropelle[b,d], Everardo M. Carneiro[b,c], Joseane Morari[a,b], Licio A. Velloso[a,b,*]

[a] Laboratory of Cell Signaling, University of Campinas, 13083-865 Campinas, SP, Brazil
[b] Obesity and Comorbidities research Center, University of Campinas, 13083-865 Campinas, SP, Brazil
[c] Department of Structural and Functional Biology, University of Campinas, 13083-865 Campinas, SP, Brazil
[d] CEPECE - Research Center of Sport Sciences, School of Applied Sciences, University of Campinas, Limeira, SP, Brazil

ARTICLE INFO

*Keywords:*
Inflammation
Hypothalamus
Diabetes
Glucose
CCBP2

ABSTRACT

In experimental obesity, the hypothalamus is affected by an inflammatory response activated by dietary saturated fats. This inflammation is triggered as early as one day after exposure to a high-fat diet, and during its progression, there is recruitment of inflammatory cells from the systemic circulation. The objective of the present study was identifying chemokines potentially involved in the development of hypothalamic diet-induced inflammation. In order to identify chemokines potentially involved in this process, we performed a real-time PCR array that determined Ackr2 as one of the transcripts undergoing differential regulation in obese-prone as compared to obese-resistant mice fed a high-fat diet for three days. ACKR2 is a decoy receptor that acts as an inhibitor of the signals generated by several CC inflammatory chemokines. Our results show that Ackr2 expression is rapidly induced after exposure to dietary fats both in obese-prone and obese-resistant mice. In immunofluorescence studies, ACKR2 was detected in hypothalamic neurons expressing POMC and NPY and also in microglia and astrocytes. The lentiviral overexpression of ACKR2 in the hypothalamus reduced diet-induced hypothalamic inflammation; however, there was no change in spontaneous caloric intake and body mass. Nevertheless, the overexpression of ACKR2 resulted in improvement of glucose tolerance, which was accompanied by reduced insulin secretion and increased whole body insulin sensitivity. Thus, ACKR2 is a decoy chemokine receptor expressed in most hypothalamic cells that is modulated by dietary intervention and acts to reduce diet-induced inflammation, leading to improved glucose tolerance due to improved insulin action.

## 1. Introduction

Obesity results from a chronic anabolic state characterized either by increased caloric intake or reduced energy expenditure, or yet, the association of both conditions [1,2]. Experimental studies have shown that dietary factors, particularly saturated fats, trigger an inflammatory response in the hypothalamus, which impair the activity of key neurons involved in the regulation of whole body energy status [3–7]. TLR4 signaling and the induction of endoplasmic reticulum stress are the triggers of the molecular machinery that connect the increased consumption of dietary fats with the installation of hypothalamic inflammation [4,6,7]. In addition, studies have provided evidence for the involvement of resident microglia and astrocytes as the cellular components of this inflammatory process [8–12]. The hypothesis that, upon induction of hypothalamic inflammation, peripheral immune cells could be recruited to the hypothalamus in order to expand the inflammatory response is currently under intense investigation. In this context, it was demonstrated that the chemokine CX3CL1 (fractalkine) is rapidly induced in the hypothalamus following the introduction of a high-fat diet (HFD) and acts as a mediator for the recruitment of bone marrow derived cells to expand the hypothalamic microglia involved in the generation of inflammation [8]. Moreover, a recent study has provided a detailed characterization of the nature of peripheral monocyte migration to the hypothalamus [9].

☆ The Laboratory of Cell Signaling belongs to the National Institute of Science and Technology – Neuroimmunomodulation (INCT-NIM)

* Corresponding author at: LAV, Laboratory of Cell Signaling, 1084-970 Campinas, SP, Brazil.
*E-mail address:* lavelloso@fcm.unicamp.br (L.A. Velloso).

https://doi.org/10.1016/j.bbadis.2019.01.001
Received 23 July 2018; Received in revised form 6 December 2018; Accepted 2 January 2019
Available online 07 February 2019
0925-4439/ 

In most chronic inflammatory conditions, a network of cytokines and chemokines play important roles in the initiation and maintenance of the inflammatory activity [13]. With this concept in mind, we hypothesized that chemokines other than fractalkine could be induced in the hypothalamus during early diet-induced obesity and play important roles in the metabolic outcomes of obesity. To test this hypothesis, we determined the landscape of cytokines/chemokines expressed in the hypothalamus of mice fed a HFD, comparing obesity-resistant (OR) versus obesity-prone (OP) mice. We identified the decoy chemokine receptor Ackr2 as one of the transcripts with greatest difference between the two groups, becoming significantly reduced in the hypothalamus of OP mice as early as three days after the introduction of a HFD. The hypothalamic lentiviral overexpression of ACKR2 reduced diet-induced hypothalamic inflammation and reduced obesity-associated glucose intolerance. Thus, the abnormal expression of ACKR2 in the hypothalamus of OP mice may contribute to defective whole body glucose tolerance.

## 2. Results

### 2.1. Hypothalamic expression of Ackr2 is differentially regulated in obese-prone and obese-resistant mice

In the first part of the study, we aimed at identifying transcripts encoding for chemokine or chemokine-related proteins that could be differentially regulated in the hypothalamus of OP and OR mice fed a HFD. For that, mice were fed a HFD for three days, and hypothalamic transcripts were evaluated using a real-time PCR array. Out of 84 transcripts (Supplementary Table 1) evaluated in the array, 18 presented at least a 2-fold differential expression as compared to control in at least one of the conditions, OP or OR (Fig. 1A). Ackr2 expression underwent a > 2-fold increase in OR mice and 1.5-fold increase in OP mice (Fig. 1A). In real-time PCR experiments performed in OP and OR mice fed either chow or HFD for three days, hypothalamic Ackr2 transcript was significantly lower in OP mice fed a HFD as compared to respective control (Fig. 1B). CCL2 and CCL5 are chemokines known to be potentially scavenged by ACKR2; in the PCR array, we detected an increase in the expression of CCL5, but not CCL2, in the hypothalamus of OP, but not OR mice fed on a HFD for three days (Supplementary Table 2).

### 2.2. ACKR2 is widely expressed in the hypothalamus of mice

Because virtually no previous study has evaluated the expression of ACKR2 in the hypothalamus, we employed immunofluorescence staining to determine the cellular and anatomical distribution of ACKR2 in the hypothalamus. The experiments revealed that ACKR2 is expressed in neurons and glia. Specifically, ACKR2 was present in NPY (Fig. 2A) and POMC (Fig. 2B) neurons and in astrocytes (Fig. 3A) and microglia (Fig. 3B). Negative controls are depicted in Supplementary Fig. 1.

### 2.3. Increased expression of ACKR2 in the hypothalamus does not modify caloric intake and body mass of mice

In order to evaluate the impact of increasing hypothalamic ACKR2, mice were submitted to the protocol as depicted in Fig. 4A and a number of parameters were determined. The lentiviral approach promoted a significant increase in the expression of Ackr2/ACKR2 transcripts (Fig. 4B) and activation of signaling through cofilin (Fig. 4C) in the hypothalamus of mice. However, this was not accompanied by changes in daily caloric intake (Fig. 4D), cumulative caloric intake (Fig. 4E), and body mass gain (Fig. 4F).

### 2.4. Increased expression of ACKR2 in the hypothalamus reduces diet-induced inflammation

Because hypothalamic inflammation is an important outcome of the consumption of a HFD, which contributes to neuronal dysfunction leading to anomalous regulation of caloric intake and energy expenditure, we evaluated the impact of the overexpression of ACKR2 in the hypothalamus on the expression of inflammatory genes. Both in OR and OP mice, the increased hypothalamic expression of Ackr2 reduced the expression of TNF-α (Fig. 5A), IL-1β (Fig. 5B), IL-10 (Fig. 5D), F4/80 (Fig. 5G), MCP1 (Fig. 5H) and, in OR mice, the receptor for fractalkine, CX3CR1 (Fig. 5J). No changes were detected in the expressions of IL6 (Fig. 5C), IL17R (Fig. 5E), Cd11b (Fig. 5F), fractalkine, CX3CL1 (Fig. 5I) and CD36 (Fig. 5K). IL17 transcripts were not detected in the hypothalamus (not shown).

### 2.5. Increased expression of ACKR2 in the hypothalamus improves glucose tolerance in obesity-prone mice

In OP mice (but not in OR mice, not shown), increased expression of ACKR2 in the hypothalamus was accompanied by reduction of blood glucose levels during a GTT (Fig. 6A and B). This was also accompanied by a reduction of blood insulin levels during the GTT (Fig. 6C). In addition, in OP mice (but not OR mice, not shown), the overexpression of ACKR2 in the hypothalamus was accompanied by reduced insulin AUC during an ITT (Fig. 6D and E) and improved insulin action as determined by the determination of the kITT (Fig. 6F). In the liver, the expression of G6pase was not affected, but Pepck was significantly reduced in OP mice treated with the lentivirus overexpressing ACKR2 (Fig. 6G and H). Insulin secretion from isolated pancreatic islets was reduced in OP mice, but not OR mice treated with the lentivirus that overexpressed Ackr2 in the hypothalamus (Fig. 6I). This was

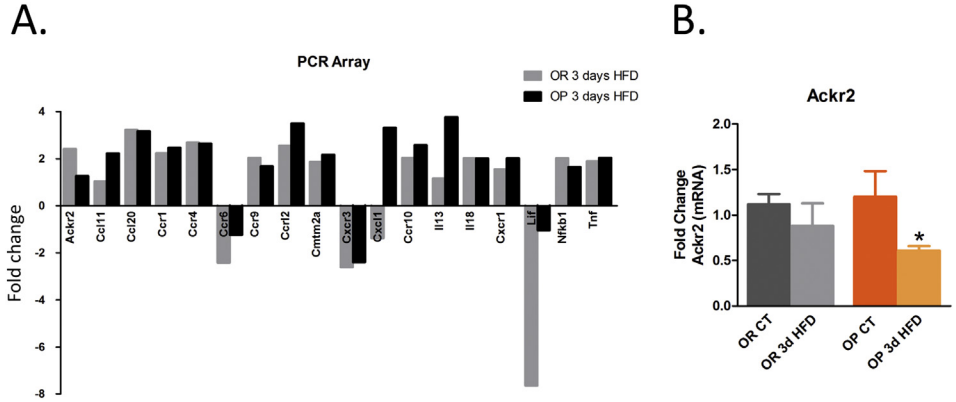


**Fig. 1.** Transcript expression in the hypothalamus. A, The cDNA prepared from hypothalamic RNA was employed in a real-time PCR array to measure transcript expression levels in control mice fed chow, in obesity-prone (OP) and obesity-resistant (OR) mice fed a high-fat diet (HFD) for three days; only the transcripts undergoing significant difference from control are presented; the results are presented as fold-change relative to chow; the identity of the transcripts is presented in Supplementary Table 1. B, The relative expression of Ackr2 transcript was determined by real-time PCR in hypothalamic samples from control mice fed on chow or OP and OR mice fed on chow (CT) or HFD for three days; the results are presented as fold-change relative to control mice. In A, n = 3; in B, n = 5; *p < 0.05 vs. OP CT.

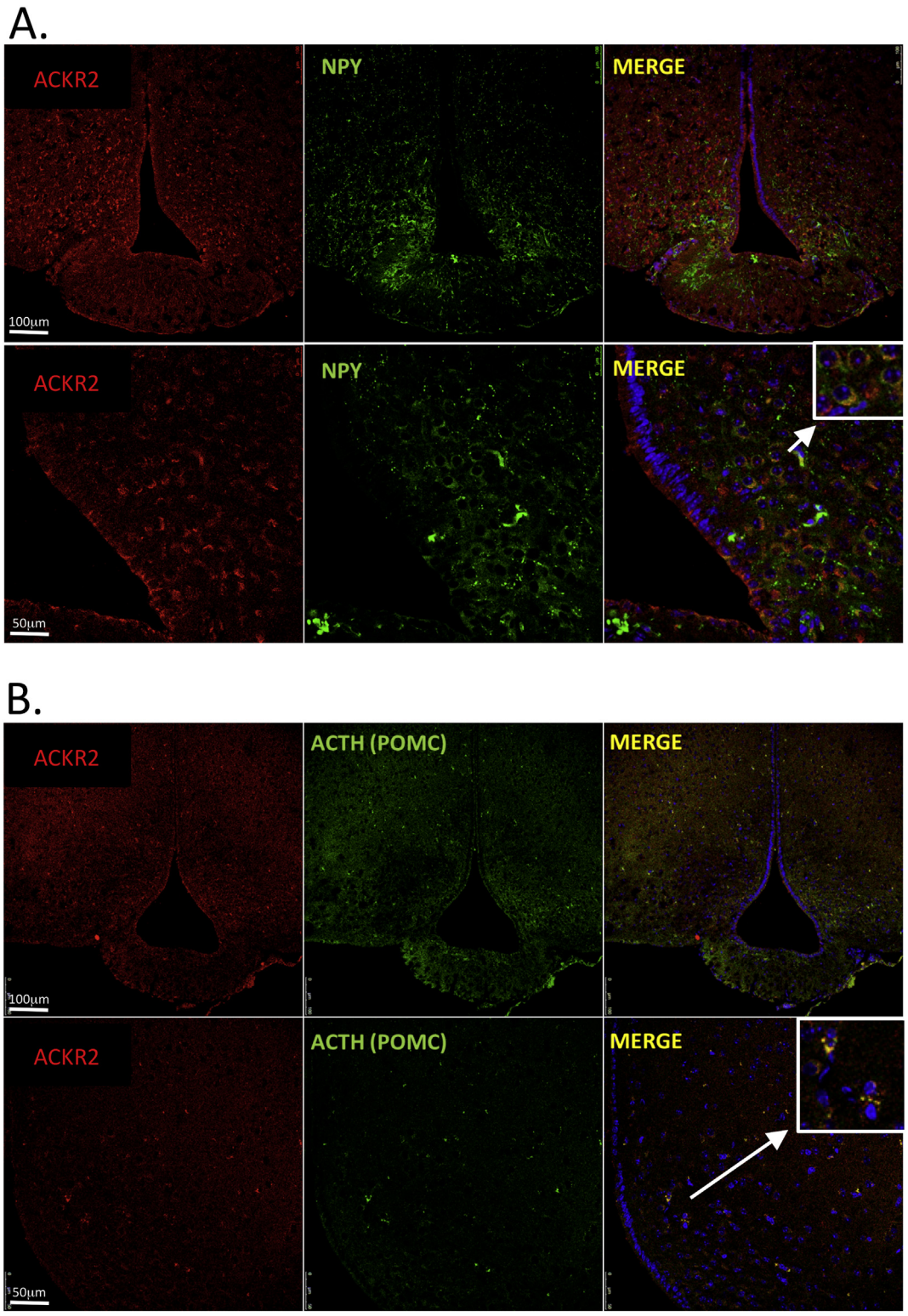


**Fig. 2.** The anatomical and cellular distribution of ACKR2 in the hypothalamus of mice. Frozen hypothalamic sections (5.0 µm) were prepared from 6-week-old mice fed on chow. Immunofluorescence staining was performed using antibodies against ACKR2 (A-B), NPY (A), and ACTH (POMC precursor, B). Nuclei were labeled using DAPI. In some panels, a high magnification image depicts details of cells (arrows). Color codes and magnifications are presented in the panels. Figures are representative of three independent experiments.

accompanied (Fig. 7A–D) by a reduction in the proportion of small islets (0–5 $\mu m^2$) and an increase in the proportion of medium-size islets (5–15 $\mu m^2$) in OP mice overexpressing ACKR2 in the hypothalamus (Fig. 7C and D). In OR mice, the overexpression of ACKR2 in the hypothalamus resulted in no significant changes in pancreatic islet size (Fig. 7A and B).

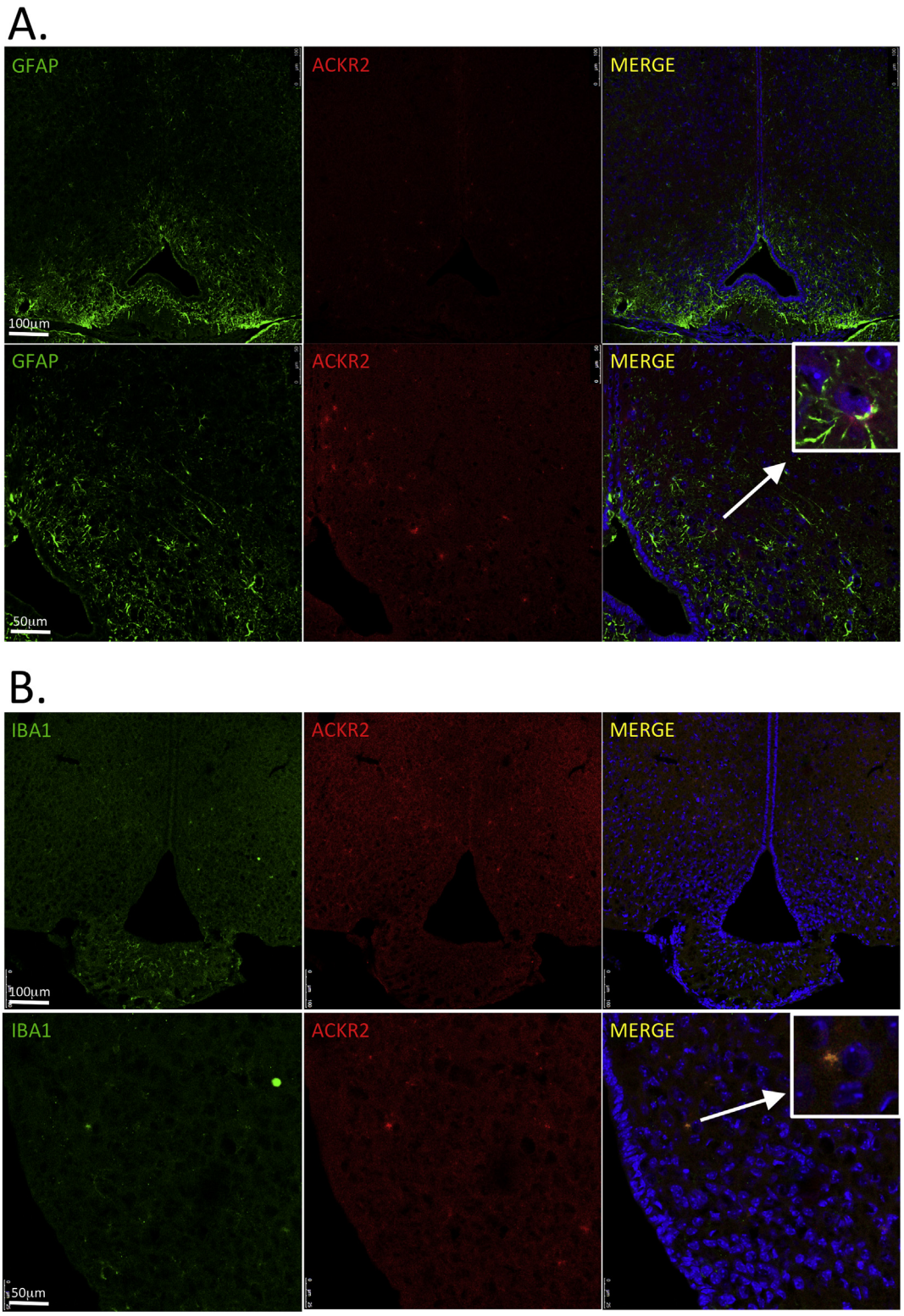


**Fig. 3.** The anatomical and cellular distribution of ACKR2 in the hypothalamus of mice. Frozen hypothalamic sections (5.0 µm) were prepared from 6-week-old mice fed on chow. Immunofluorescence staining was performed using antibodies against ACKR2 (A–B), GFAP (A), and IBA-1 (B). Nuclei was labeled using DAPI. In some panels, a high magnification image depicts details of cells (arrows). Color code and magnifications are presented in the panels. Figures are representative of five independent experiments.

### *2.6. Bioinformatics analysis provides further evidence for the association of hypothalamic Ackr2 and systemic glucose control*

Using a public dataset, we compared the hypothalamic transcript expression of Ackr2 with the hepatic expression of proteins involved in the regulation of systemic glucose levels. As depicted in Fig. 8A, selecting the mice families with the highest and lowest hypothalamic Ackr2, we found concordance with enzymes involved in glycolysis and glycogen synthesis, such as glycogen synthase 2 (Gys2), phosphoglucomutase 2 (Pgm2), glucokinase regulator (Gckr), and glucokinase

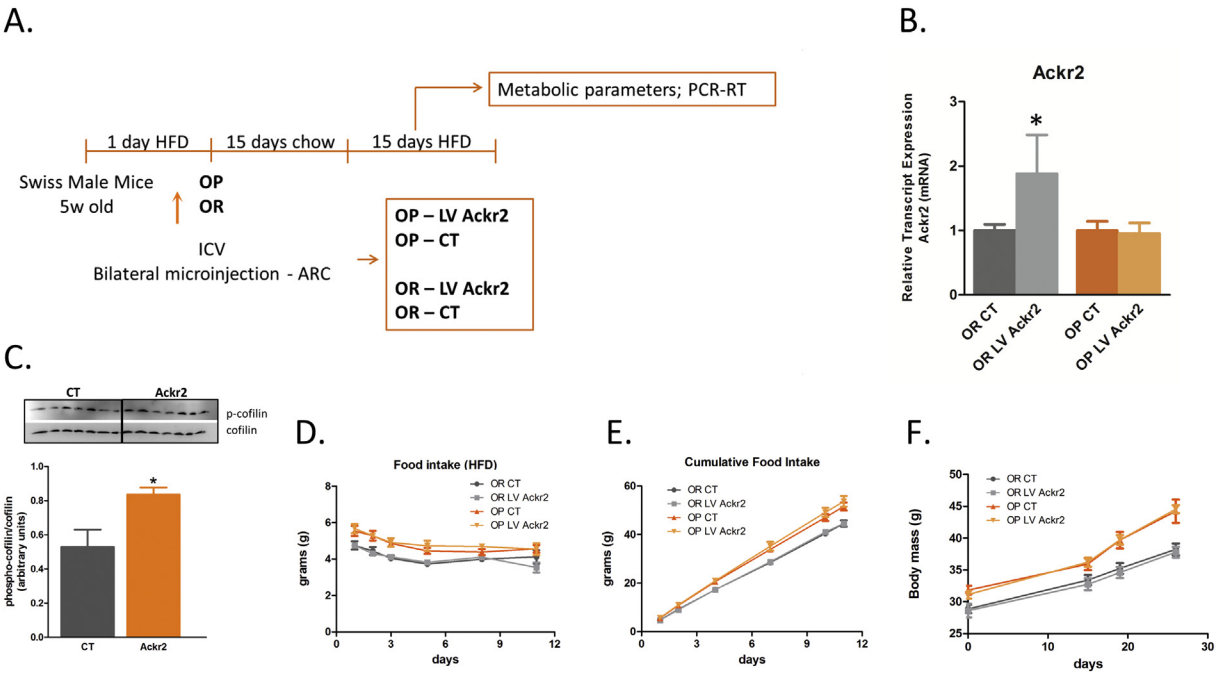


**Fig. 4.** Body mass and caloric intake outcomes of overexpressing ACKR2 in the hypothalamus of mice. A, Schematic representation of the protocol employed to overexpress ACKR2 in the hypothalamus of obese-prone (OP) and obese-resistant (OR) mice using a lentivirus (LV Ackr2) microinjected bilaterally in the arcuate nucleus (ARC). B, The expression of Ackr2 transcript was determined by real-time PCR. C, The activation of ACKR2 was determined by immunoblot using an antibody against p-cofilin. Spontaneous daily food intake (D); cumulative food intake during the experimental period (E); and, body mass during the experimental period (F) in mice submitted to the ACKR2 overexpression protocol. In all experiments n = 4–6; *p < 0.05 vs. respective control.

(Gck); whereas discordance was found for phosphoenolpyruvate carboxykinase 1 (Pck1), which plays a pivotal role in gluconeogenesis. Moreover, there was also discordance between hypothalamic Ackr2 and the systemic glucose/insulin ratio. The inverse and direct correlations of Ackr2 with Pck1 and Gys2, respectively, were further evidenced by an expanded analysis including all families of mice with available data (Fig. 8B). Finally, in Persons' rank analysis, we confirmed a high direct correlation between hypothalamic Ackr2 and Gys2, Pgm2, Gckr, and Gck (Fig. 8C), whereas a negative correlation was found for Pck1 and the phenotype glucose/insulin ratio (Fig. 8C).

## 3. Discussion

Diet-induced hypothalamic inflammation is a hallmark of experimental obesity [1,2]. Here, we investigated chemokine and chemokine-related proteins that could be involved in obesity predisposition by affecting the magnitude of the inflammatory process in the hypothalamus of mice fed a HFD. We show that ACKR2, a decoy chemokine receptor, is induced in the hypothalamus early after the introduction of a HFD both in OP and OR mice; however, in OP mice, the increment of ACKR2 is significantly smaller that in OR mice. Using a lentivirus, we obtained significant increase in hypothalamic ACKR2, which was accompanied by reduced diet-induced hypothalamic inflammation and improved systemic glucose tolerance without affecting caloric intake and body mass.

ACKR2 belongs to a small subset of chemokine receptors identified as atypical chemokine receptors, hence the acronym ACKR [14]. According to the HUGO Gene Nomenclature Committee (genenames.org), currently, there are six genes encoding ACKR proteins, namely ACKR1-4, CCRL2, and PITPNM3. Recently, it has been requested that CCRL2 and PITPNM3 be renamed as ACKR5 and ACKR6, respectively, but approval is still pending [15]. Except for PITPNM3, all members of this family exhibit a predicted seven-transmembrane-domain structure; however, none of them is capable of activating signal transduction through the Gi protein [14]. The lack of chemotactic activity and the capacity of scavenging chemokines are the main functional features that characterize the ACKRs [14,15]. Particularly for ACKR2, studies have shown that it can scavenge CCL2-5, CCL3L1, CCL7-8, CCL11, CCL13-14, CCL17, and CCL22 [14,15]. As an important outcome of chemokine scavenging, reduction of inflammatory activity has been reported in different tissues and different experimental and clinical contexts [14,15].

Only a few studies have evaluated the roles of ACKR2 in neuroinflammatory conditions [16,17]. In experimental autoimmune encephalomyelitis, there are controversial data regarding the involvement of ACKR2 in the pathophysiology of the disease [16,17]. Thus, Hansell and coworkers [16] have shown that in the absence of ACKR2, mice develop a more pronounced clinical expression of the condition, which is accompanied by increased expression of IL-17 and increased number of B-lymphocytes expressing granulocyte-macrophage colony-stimulating factor, which is strongly suggestive of enhanced inflammatory activity; conversely, Liu and coworkers [17] have shown that ACKR2 knockout mice exhibit a protective phenotype against the development of autoimmune encephalomyelitis, which was characterized by attenuated interferon-gamma production. No previous study has evaluated the expression and potential roles of ACKR2 in the hypothalamus.

In the present study, we showed that there were two major outcomes of the increased expression of ACKR2 in the hypothalamus of mice: i) reduction of diet-induced hypothalamic inflammation and ii) improvement of systemic glucose tolerance. As a decoy receptor that can scavenge a number of chemokines, it was expected that upon increased ACKR2 expression, the inflammatory activity in the hypothalamus could be dampened. Out of the chemokines that can potentially be scavenged by ACKR2, only two, CCL2 and CCL5, have been reported to play a role in hypothalamic function in obesity/diabetes [8,18]. CCL2 expression is increased in the hypothalamus of rodents fed a HFD [8,18] and approaches aimed at reducing the inflammatory activity, such as inhibition of fractalkine [8] or treatment with n3-polyunsaturated fatty acids (PUFAs) [18] result in the reduction of hypothalamic CCL2. Similarly, CCL5 is increased in the hypothalamus of

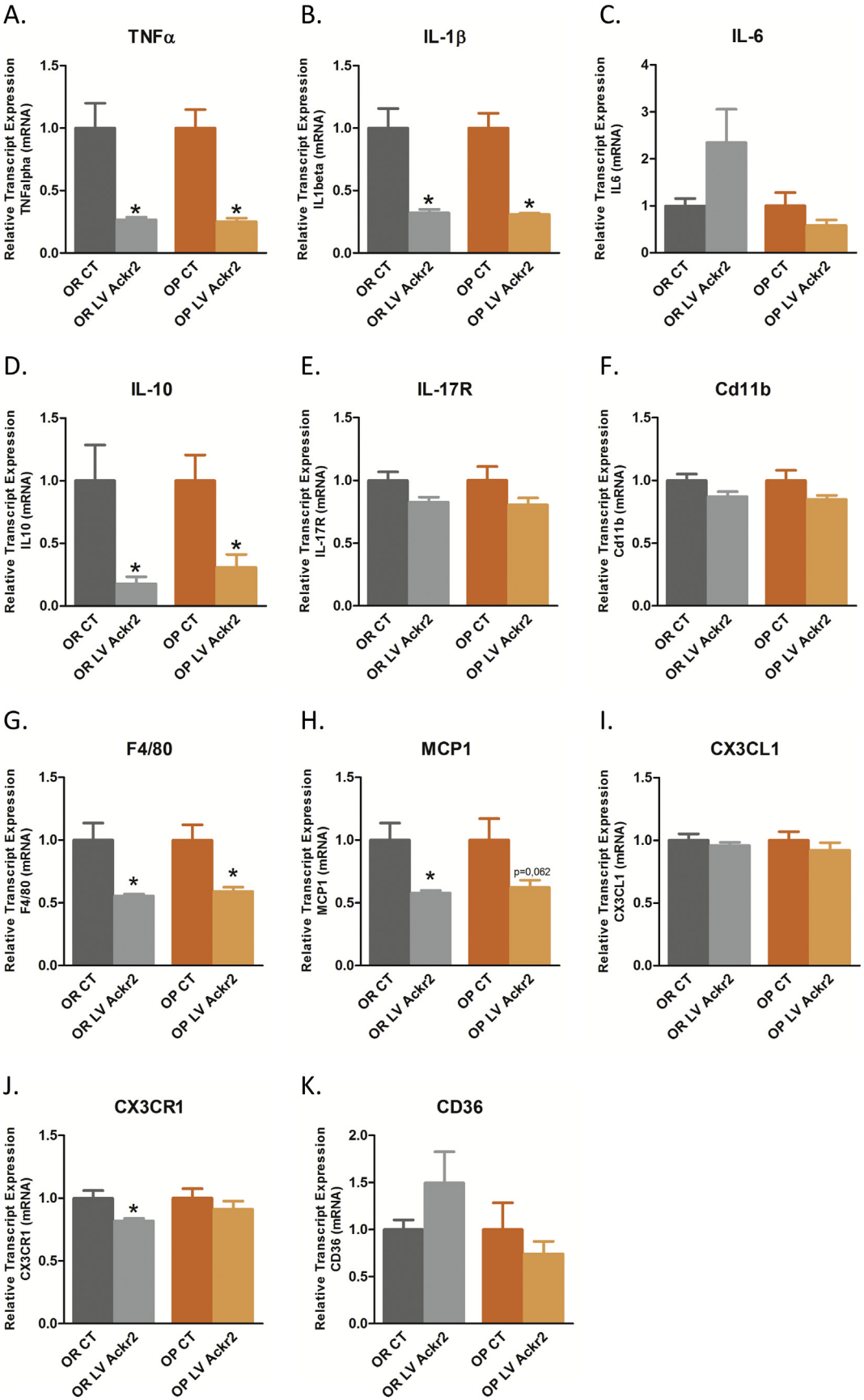


**Fig. 5.** Impact of overexpressing hypothalamic ACKR2 on inflammatory markers. A–K, Real-time PCR was employed to determine the relative expression of transcripts encoding for TNF-α (A), IL-1β (B), IL-6 (C), IL-10 (D), IL17R (E), Cd11b (F), F4/80 (G), MCP1 (H), CX3CL1 (I), CX3CR1 (J) and CD36 (K) in the hypothalamus of obesity-prone (OP) and obese-resistant (OR) mice injected with a lentivirus designed to increase ACKR2 expression (LV Ackr2) or a control lentivirus (CT). In A–H, n = 5; *$p < 0.05$ vs. CT.

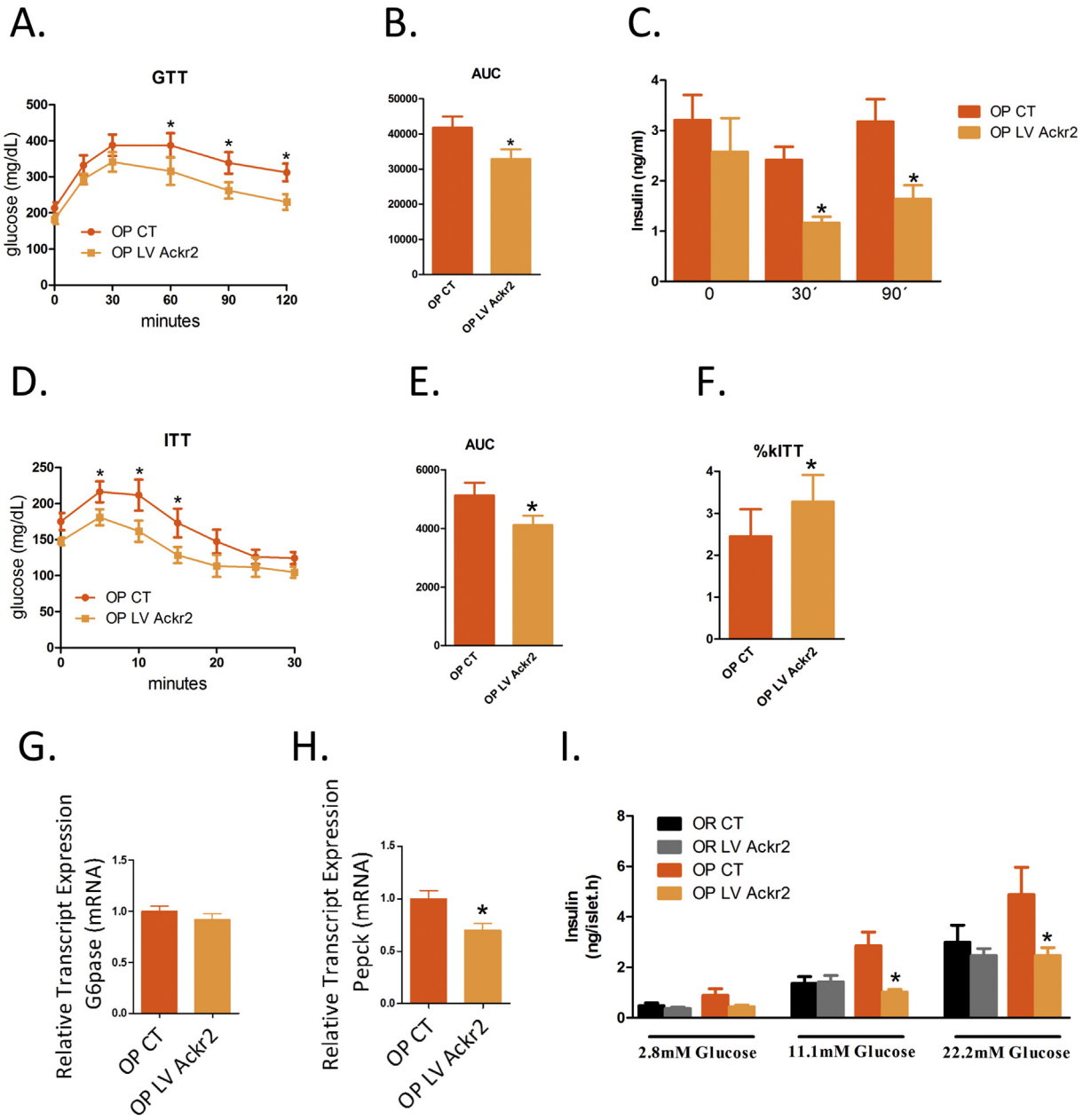


**Fig. 6.** Impact of overexpressing hypothalamic ACKR2 on systemic glucose tolerance. Mice were treated according to the protocol presented in Fig. 4A and parameters were determined at the end of the experimental period. In the glucose tolerance test (GTT), blood glucose variation was measured from time 0 to 120 min (A) and the area under the curve (AUC) for glucose was calculated (B); in addition, during the GTT, blood insulin was determined at times 0, 30, and 90 min (C). In the insulin tolerance test (ITT), blood glucose variation was measured from time 0 to 30 min (D), the area under the curve (AUC) for glucose was determined (E), and the constant for glucose decay (kITT) was calculated (F). In the liver, real-time PCR was employed to determine the relative expression of transcripts encoding for G6pase (G) and Pepck (H). The static secretion of insulin was determined in isolated pancreatic islets exposed to 2.8, 11.1, or 22.2 mM glucose (I). In all experiments n = 5; *$p < 0.05$ vs. respective control condition.

diet-induced obese mice, and treatment with n3-PUFAs reduces its expression [18]; however, at least one study has shown that genetic disruption of the hypothalamic CCL5/CCR5 system leads to systemic glucose intolerance by a mechanism dependent on AMPK-dependent insulin sensing in the hypothalamus [19], suggesting that CCL5 has a beneficial effect on hypothalamic control of systemic metabolism. In the present experimental setting, the increased expression of ACKR2 in the hypothalamus resulted in reduction in the expression of two inflammatory cytokines, TNF-α and IL-1β; one marker of microglia, F4/80; and two markers of chemotaxis, MCP1 and the receptor for fractalkine, CX3CR1. Interestingly, the expression of IL6 was not affected by the overexpression of hypothalamic ACKR2. IL6 can have both pro- and anti-inflammatory actions depending of the anatomical region and context; and, particularly in the hypothalamus, studies have shown that IL6 can act as a protective factor against diet-induced inflammation. Thus, we believe that under increased expression of ACKR2, the fact that IL6 expression was not down-regulated could be an additional evidence of reduced inflammation.

Surprisingly, despite the fact that increasing hypothalamic ACKR2 reduced the expression of several markers of inflammation in the hypothalamus, this was not accompanied by reduced caloric intake and body mass. In many studies using genetic and/or pharmacological approaches to reduce hypothalamic inflammation in different experimental models of obesity, the reduction of caloric intake and body mass

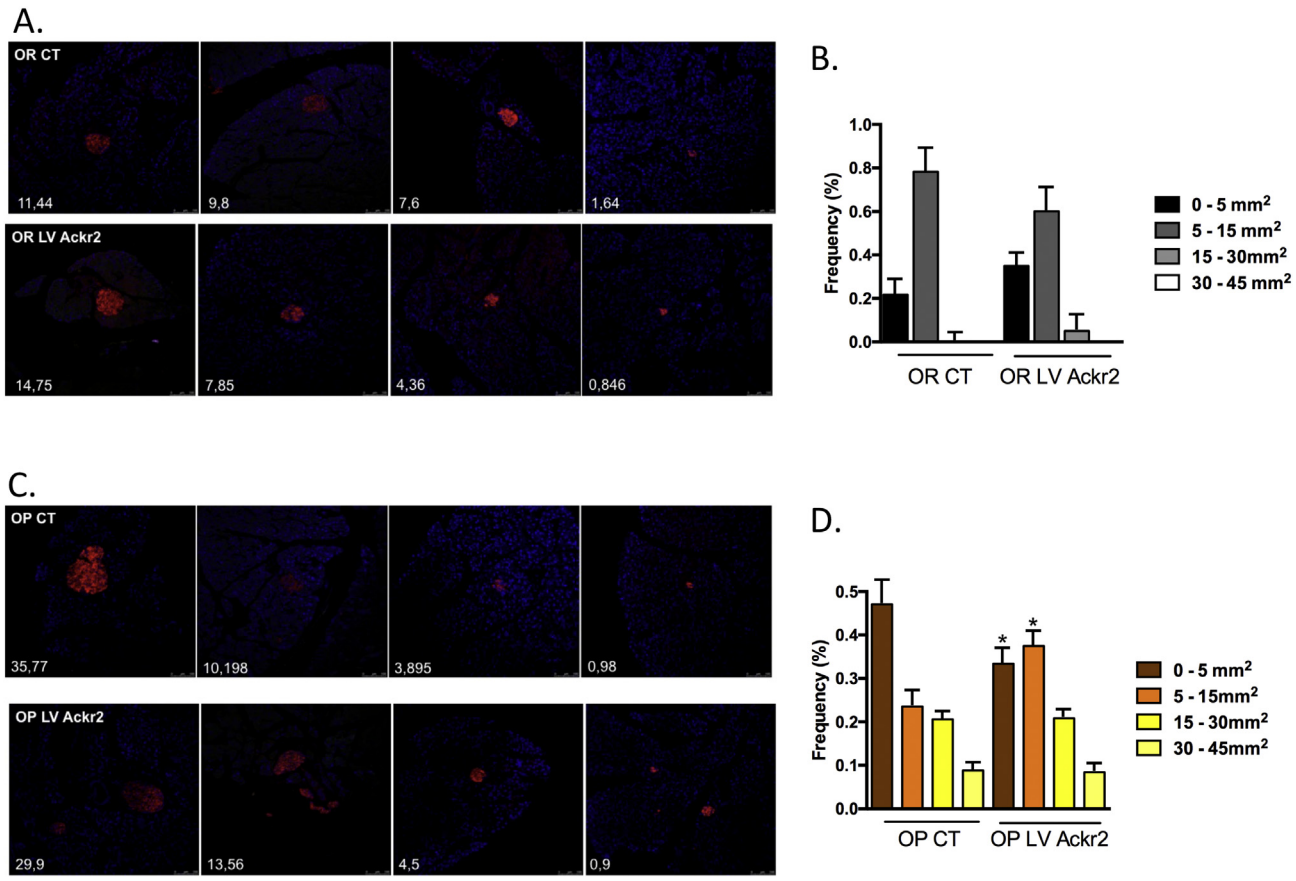


**Fig. 7.** Impact of overexpressing hypothalamic ACKR2 on pancreatic islet size. Mice were treated according to the protocol presented in Fig. 4A and pancreases were harvested for immunofluorescence staining with anti-insulin antibodies (red) followed by the determination of pancreatic islet area; DAPI (blue) was employed for nuclear staining. A and C depict representative images of pancreatic islets in control (CT) and Ackr2 lentivirus (LV Ackr2) treated obese-resistant (OR) (A) and obese-prone (OP) mice. Islets were categorized according to the area and the frequencies of islets in each area range are depicted in B (OR mice) and D (OP mice). In all experimental conditions, a total of seven pancreatic sections from four pancreases were used in the experiments. In A and C, the numbers in the left-hand bottom corners indicate the area of the islet depicted in the respective image. In D, *$p < 0.05$ vs. respective area range in OP CT.

was obtained [8–12]. However, it is currently known that the distinct subpopulations of hypothalamic neurons involved in the control of systemic metabolism and energy homeostasis exert specific functions with a certain degree of specialization. Thus, whereas POMC neurons of the arcuate nucleus are mostly involved in the control of postprandial satiety and systemic glucose levels [20–22], AgRP neurons exert robust control of long-term whole body energy stores [23]. Yan and coworkers showed that both in obesity and ageing, the production of TGF-β by hypothalamic astrocytes could affect POMC neurons by a mechanism dependent on RNA stress leading to an abnormal neural regulation of hepatic gluconeogenesis [22]. In addition, we have previously shown that reduction of diet-induced hypothalamic inflammation by inhibiting either TNF-α or TLR4 restores obesity-associated abnormal hepatic gluconeogenesis by a mechanism dependent of parasympathetic signaling to the liver [24]. Thus, it could be hypothesized that the protective effect of ACKR2 during the development of obesity-associated hypothalamic inflammation is mostly reflected in the activity of neurons involved in systemic glucose homeostasis rather than caloric intake and body mass.

Hypothalamic neurons can control systemic glucose levels by modulating insulin secretion and hepatic glucose production through autonomic connections [20,24]. Here, we showed that increasing hypothalamic ACKR2 in experimental obesity resulted in improved glucose tolerance due to enhanced insulin sensitivity. Thus, during the GTT, there was a significant reduction of glucose levels accompanied by reduced blood insulin; and, in the ITT, glucose levels were reduced whereas the kITT was increased. Moreover, insulin secretion from isolated pancreatic islets was reduced. Taken together, these results suggest that the improved systemic insulin responsiveness promoted increased glucose tolerance and impacted pancreatic islets due to the reduced peripheral demand for insulin. Because attenuated hypothalamic inflammation can reduce hepatic glucose production [20,24], we determined the levels of enzymes that play pivotal roles in liver gluconeogenesis; in fact, we showed that increasing hypothalamic ACKR2 was accompanied by reduction of Pepck. To further explore this finding, we took advantage of a bioinformatics analysis using a public dataset from BXD mice families [25]. The analysis confirmed the existence of an inverse relation between hypothalamic Ackr2 and hepatic gluconeogenic enzyme PEPCK, and also an inverse relation with systemic glucose/insulin ratio. Furthermore, the analysis provided strong evidence for a direct relation between hypothalamic Ackr2 and a number of enzymes involved in hepatic glycogen synthesis.

In conclusion, this is the first study showing that the decoy chemokine receptor ACKR2 is increased in the hypothalamus during obesity. The magnitude of its expression is smaller in mice that are prone to obesity as compared to mice resistant to obesity. Upon induction of ACKR2 in the hypothalamus of OP mice, there is reduction of hypothalamic inflammation and improved systemic glucose homeostasis. Thus, ACKR2 emerges as a new immunomodulatory player in the context of diet-induced hypothalamic inflammation and methods aimed at increasing its hypothalamic expression may be useful for improving metabolic control in obesity.

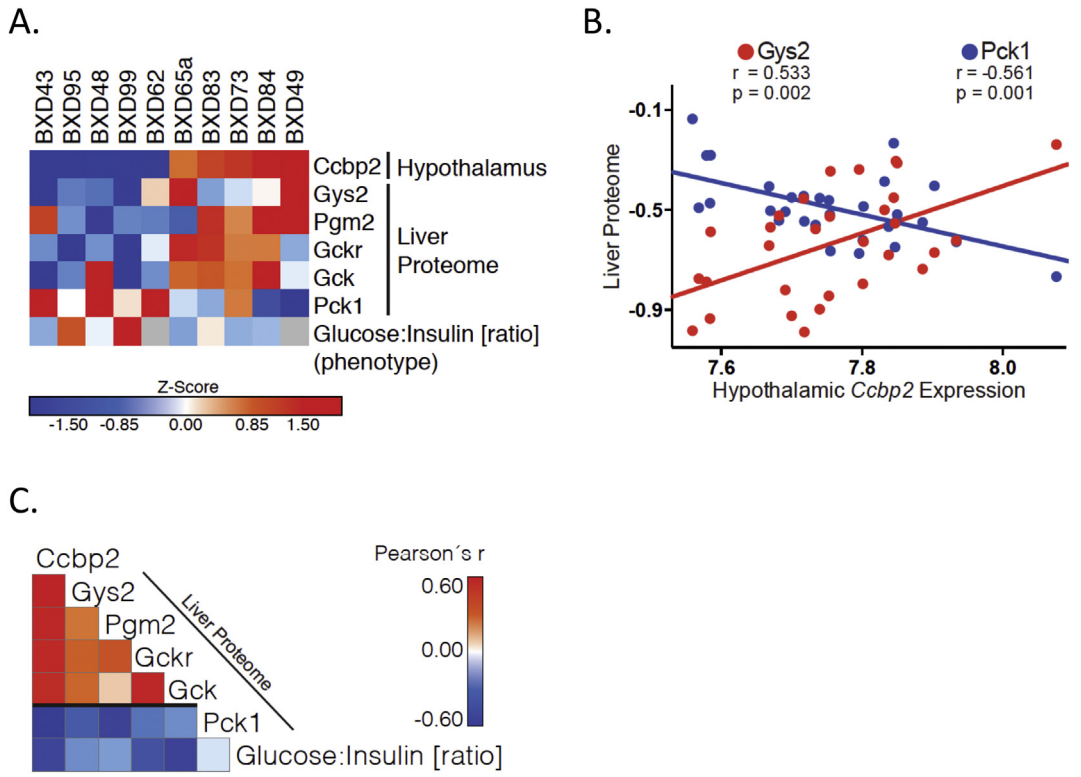


**Fig. 8.** Bioinformatics analysis of the correlation between hypothalamic Ackr2 transcripts and parameters related to systemic glucose regulation. A. Heatmap showing the correlation between hypothalamic Ackr2 (Ccbp2) transcripts and liver proteins involved in glucose regulation; hypothalamic Ackr2 was also confronted with the glucose/insulin ratio phenotype; the heatmap includes only the data from mice families presenting the highest and lowest levels of hypothalamic Ackr2. B, Graphic representation of the correlation between hypothalamic Ackr2 transcripts and liver glycogen synthase 2 (Gys2) or phosphoenolpyruvate carboxykinase (Pck1) in all mice families. C, Corrgram showing the positive (red) and negative (blue) correlations between hypothalamic Ackr2 and liver proteins involved in glucose regulation and also with glucose/insulin ratio; data form all mice families. Gck, glucokinase; Gckr, glucokinase regulator; Pgm2, phosphoglucomutase 2.

## 4. Methods

### 4.1. Experimental animals

Male Swiss mice were obtained from the University of Campinas Breeding Center and the study was approved by the Ethics Committee of the University of Campinas (Project #: CEUA 2926-1). In all experiments, 5-week-old mice were maintained in individual cages with controlled temperature (24–26 °C) under a 12 h light/dark cycle (lights on at 6 AM; lights off at 6 PM). Mice had free access to water and food ad libitum. To identify OP and OR mice, we employed a protocol previously described [26]. In summary, mice were fed a high-fat diet (HDF) for 24 h and grouped into quartiles for total food intake. The top of quartile was defined as OP and the bottom of quartile as OR mice. Each group started with 20 mice and resulted in the selection of five OP and five OR mice. Thereafter, mice were randomly selected for an intracerebroventricular injection of a lentivirus containing the Ackr2 hairpin or a control lentivirus. Fifteen days after lentivirus delivery, mice were transferred to a HFD (composition of diets in Table 1) and experiments were performed after 15 days. Body mass and caloric intake were determined every second day.

**Table 1**
Macronutrient composition of the diets.

| | Control - chow | | High-fat diet - HFD | |
|---|---|---|---|---|
| | g% | kJ% | g% | kJ% |
| Protein | 19 | 18 | 19 | 12 |
| Carbohydrates | 77 | 73 | 45 | 27 |
| Lipids | 4 | 9 | 36 | 61 |
| kJ/g | | 15.8 | | 24.5 |

### 4.2. PCR array

The PCR array was performed using RNA prepared from the hypothalami of OP and OR mice fed a HFD for three days. The kit used for determination of gene expression was Chemokines & Receptors PCR Array (PAMM-022Z, Qiagen). This is a 96-gene panel, with 84 genes for chemokines/chemokine receptors.

### 4.3. Lentiviral production for Ackr2 overexpression

For the production of the lentivirus, HEK 293T cells were transfected with the following protocol: 200 µL of DMEM was added with 12 µL of Fugene (in the Fugene:DNA ratio of 3:1); after 5 min of incubation, 2 µg of the hairpins for Ackr2 overexpression were added, along with 1.8 µg of the ampicillin resistance plasmid VPR and 0.2 µg of the VSV-G protein envelope. This mix was distributed on plates containing HEK cells with confluence of 80% to 90% in DMEM with 10% fetal bovine serum and penicillin/streptomycin. After 24 h, the culture medium was replaced by a fresh medium with 30% fetal bovine serum. After 48 h, the culture medium was collected and passed through a 0.45-µm filter and frozen for later use. The lentivirus for overexpression of the chemokine Ackr2 is GFP+.

### 4.4. Hypothalamic microinjection of Ackr2 lentivirus

OP and OR mice were randomly selected for the treatment with Ackr2 lentivirus (LV Ackr2) or control lentivirus (CT). For that, mice were anesthetized with a mixture of ketamine (100 mg/kg) and xilazin (10 mg/kg). An interparietal incision was performed, and the skull was

exposed, allowing the identification of the bregma. Microinjection followed the stereotaxic coordinates for the arcuate nucleus: depth 4.5 mm; lateral + and – 0.3 mm; antero-posterior: – 1.7 mm. Lentivirus (1.0 μL) were injected into both hemispheres of the hypothalamus.

### 4.5. Glucose tolerance test (GTT)

A 25% glucose solution was injected intraperitoneally in 4-h fasted mice. Glucose measurements occurred at times 0, 15, 30, 60, 90, and 120 min. The measurements were performed in blood from the tail using a portable glucose meter (Optium Xceed - Abbott®). Thereafter, the area under the curve (AUC) for glucose was calculated. To measure blood insulin during the GTT, blood samples were collected at 0, 30, and 90 min. ELISA (EMD, Millipore) was employed to determine the levels of insulin.

### 4.6. Insulin tolerance test (ITT)

The ITT was performed in 4-h fasted mice. Tail vein blood was collected immediately before the intraperitoneal injection of insulin (1.5 IU/kg body mass) and after 5, 10, 15, 20, 25, and 30 min. Glucose was determined using a portable glucose meter (Optium Xceed - Abbott®). Thereafter, the area under the curve (AUC) for glucose and the constant for glucose decay during the ITT (kITT) were calculated.

### 4.7. Real-time PCR

Reactions were performed using the TaqManTM System (Applied Biosystems). The transcript of glyceraldehyde-3-phosphate dehydrogenase (GAPDH) was elected as the endogenous control for the reaction. The expressions of Ackr2 (Mm00445551_m1), TNF-α (Mm00443258_m1), interleukin (IL)-1β (Mm00434228_m1), IL-6 (Mm00446190_m1), IL-10 (Mm01288386_m1), IL17R (Mm00434214_m1), CD11b (Mm00434455_m1), F4/80 (Mm00802529_m1), MCP1 (Mm99999056_m1), CX3CL1 (Mm0436454_m1), CX3CR1 (Mm00438354_m1) and CD36 (Mm01135198_m1) transcripts were quantified in the hypothalamus. For the determination of relative transcript expression, real-time PCR reactions were performed in duplicates, as follows: 3.0 μL TaqMan Universal PCR Master Mix 2×, 0.25 μL of primers and probe solution, 2.75 μL water, and 4.0 μL cDNA. The values of relative gene expression were obtained by analyzing the results in the 7500 System SDS software (Applied Biosystems).

### 4.8. Immunohistochemistry

For hypothalamic analysis, six-week-old male Swiss mice fed on chow were anesthetized with a mixture of ketamine (100 mg/kg) and xilazin (10 mg/kg) perfused with saline and paraformaldehyde 4%. The brain was totally removed and kept during 24 h in a paraformaldehyde 4% solution, followed by 48 h in a 30% sucrose solution to be cryoprotected. The coronal sectioning, 20 μm-thickness, was performed using a cryostat (LEICA Microsystems, CM1860, Buffalo Grove, IL, USA). Sections were rinsed with PBS and blocked in a solution containing 5% normal serum, 0.2% Tween in phosphate buffered saline for 1 h at room temperature, followed by incubation at 4 °C overnight with antibodies against Ackr2 (sc67476, goat polyclonal, 1:100, Santa Cruz Biotechnology, Inc.) with IBA-1 (ab178680, rabbit polyclonal, ABCAM, 1:500, Cambridge, UK) or GFAP (ab7260, rabbit polyclonal, 1:500, ABCAM, Cambridge, UK) or ACTH (#Afp156102789, rabbit polyclonal, 1:1000) or NPY (sc133080, mouse monoclonal 1:200, Santa Cruz Biotechnology, Inc.) in a blocking buffer (1% bovine serum albumin in PBS-Tween). Next, it was incubated for 2 h with Donkey anti-goat Cy3 (ab6949, 1:500, ABCAM, Cambridge, UK) and Donkey anti-rabbit FITC (ab6798, 1:500, ABCAM, Cambridge, UK) or Donkey anti-mouse FITC (ab7057, 1:500, ABCAM, Cambridge, UK). Nuclei staining was obtained using TO-PRO®-3 Iodide ((642/661) T3605, 1:1000, Life Technologies, Carlsbad, CA, EUA) in PBS. In all experiments, negative controls performed by excluding primary or secondary antibodies. Analysis and documentation of the results were performed using fluorescence microscope confocal Leica TCS SP5 II.

### 4.9. Islet morphometry

For islet morphometric determination, pancreases (n = 4) were removed, fixed in paraformaldehyde and embedded in paraffin. From each block, 5.0 μm serial sections were obtained (every 20th section) and employed in reactions. The sections were incubated overnight with an anti-insulin (1:100; Dako North America, Inc., CA, USA), antibody at 4 °C. Subsequently, the sections were incubated with a secondary rhodamine antibody. Nuclei were stained with DAPI. We measured seven slices of each mouse. The area of islet was analyzed using the free software, Image J as previously described [27].

### 4.10. Insulin secretion

For static insulin secretion, four pancreatic islets per well were incubated 30 min with Krebs bicarbonate buffer (KBB) (115 mM NaCl, 5 mM KCl, 2.56 mM $CaCl_2$, 1 mM $MgCl_2$, 10 mM $NaHCO_3$, 15 mM HEPES, supplemented with 5.6 mM glucose, 0.3% BSA, and equilibrated with a mixture of 95% O2/5% $CO_2$ to obtain a pH 7.4). After 30 min of pre-incubation time, the medium was removed and immediately replaced with KBB containing different glucose concentrations. After 1 h of incubation time, the medium was removed and stored at −20 °C. For islet insulin content, the islets that were grouped into batches of four were handpicked and incubated overnight in an ethanol/HCl buffer at 4 °C. At the end of the incubation period, the buffer was removed, and the insulin content was analyzed. Insulin levels and total insulin content were measured by means of ELISA.

### 4.11. Bioinformatics analysis

Correlation analyses were performed using hypothalamic mRNA (INIA Hypothalamus Affy MoGene 1.0 ST [Nov10]), proteomic (EPFL/ETHZ BXD Liver, Chow Diet [Jun16] Top100 SWATH), and phenotypic data (BXD Published Phenotypes) of BXD inbred mice as previously published (Andreux, P.A. et al. Systems Genetics of Metabolism: The Use of the BXD Murine Reference Panel for Multiscalar Integration of Traits. https://doi.org/10.1016/j.cell.2012.08.012) and are accessible on GeneNetwork (www.genenetwork.org). A correlation graph was created using GraphPad Prism 5.0. Heatmaps were created using GENE-E (The Broad institute, www.broadinstitute.org/cancer/software/GENE-E/). The row values used are available in Supplementary Table 3.

### 4.12. Statistics analysis

Results are presented as the means ± standard error of the mean (SEM). For the comparison of means between two groups we used the Student *t*-test for independent samples. In GTT and ITT, curves were analyzed by one-way ANOVA and area under curves were analyzed by Student *t*-test. Linear regression test was utilized to calculate kITT (based on ITT test). The significance level was set at $p < 0.05$. Graph Pad Prism® was used to analyze the data.

## Abbreviations

ACKR2/Ackr2 atypical chemokine receptor 2
ACTH adrenocorticotrophic hormone
AgRP agouti-related protein
AUC area under the curve
CCL2 also known as MCP1, monocyte chemoattractant protein 1
CCL5 also known as RANTES, regulated on activation - normal T

| | |
|---|---|
| | cell expressed and secreted |
| CD11b | integrin alpha-M |
| CD36 | fatty acid translocase |
| CT | control |
| CX3CL1 | fractalkine |
| CX3CR1 | fractalkine receptor |
| DMEM | Dulbecco-modified Eagle medium |
| ELISA | enzyme-linked immunosorbent assay |
| F4/80 | EGF-like module-containing mucin-like hormone receptor-like 1 |
| FITC | fluorescein isothiocyanate |
| G6pase | glucose 6-phosphatase |
| GAPDH | glyceraldehyde-3-phosphate dehydrogenase |
| Gck | glucokinase |
| Gckr | glucokinase regulator |
| GFAP | glial fibrillary acidic protein |
| GFP | green fluorescence protein |
| GTT | glucose tolerance test |
| Gys2 | glycogen synthase 2 |
| HEK | human embryonic kidney |
| HFD | high-fat diet |
| IBA-1 | ionized calcium binding adaptor molecule 1 |
| IL-10 | interleukin 10 |
| IL-1β | interleukin 1 beta |
| IL-6 | interleukin 6 |
| IL-17 | interleukin 17 |
| IL-17R | interleukin 17 receptor 1A |
| ITT | insulin tolerance test |
| KBB | Krebs bicarbonate buffer |
| KITT | constant decay during the insulin tolerance test |
| LV | lentivirus |
| MCP1 | monocyte chemoattractant protein 1 |
| NPY | neuropeptide Y |
| OP | obesity-prone |
| OR | obesity-resistant |
| PBS | phosphate-buffered saline |
| PCR | polymerase-chain reaction |
| Pck1 | phosphoenolpyruvate carboxykinase 1 |
| Pepck | phosphoenolpyruvate carboxykinase |
| Pgm2 | phosphoglucomutase 2 |
| POMC | proopiomelanocortin |
| PUFA | polyunsaturated fatty acid |
| TLR4 | toll-like receptor 4 |
| TNF-α | tumor necrosis factor alpha |
| VSV-G | vesicular stomatitis virus G |

## Author contributions

MF, JM, EMC and LAV designed the experiments; MF, BB, AFR, RFM, RTH, CS, NRD, AND JFV performed the experiments; RCG and ERR performed bioinformatics analysis; MF, JM and LAV discussed and organized results; MF and LAV wrote the paper; LAV was also responsible for funding acquisition. All authors contributed to the editing and discussion of the manuscript.

## Ethics approval

The animal experiments performed in the present study were approved by the Institutional Animal Care and Use Committee (CEUA 2926-1).

## Competing interests

The authors declare that they have no competing interests.

## Transparency Document

The Transparency document associated with this article can be found, in online version.

## Acknowledgments

We thank Erika Roman, Gerson Ferraz, and Marcio Cruz from the University of Campinas for technical assistance. Grants for this study were provided by Fundação de Amparo a Pesquisa do Estado de São Paulo and Conselho Nacional de Desenvolvimento Cientifico e Tecnológico. The Laboratory of Cell Signaling belongs to the Obesity and Comorbidities Research Center and the National Institute of Science and Technology – Diabetes and Obesity.

## Funding

São Paulo Research Foundation (FAPESP – 2013/07607).

## Consent for publication under declaration

Not applicable.

## Data availability

Please contact author for data requests.

## Conflict of interest

The authors this manuscript have no conflict of interest to declare

## Appendix A. Supplementary data

Supplementary data to this article can be found online at https://doi.org/10.1016/j.bbadis.2019.01.001.

## References

[1] L.A. Velloso, M.W. Schwartz, Altered hypothalamic function in diet-induced obesity, Int. J. Obes. 35 (2011) 1455–1465.
[2] C. Cavadas, C.A. Aveleira, G.F. Souza, L.A. Velloso, The pathophysiology of defective proteostasis in the hypothalamus - from obesity to ageing, Nat. Rev. Endocrinol. 12 (2016) 723–733.
[3] C.T. De Souza, E.P. Araujo, S. Bordin, R. Ashimine, R.L. Zollner, A.C. Boschero, M.J. Saad, L.A. Velloso, Consumption of a fat-rich diet activates a proinflammatory response and induces insulin resistance in the hypothalamus, Endocrinology 146 (2005) 4192–4199.
[4] M. Milanski, G. Degasperi, A. Coope, J. Morari, R. Denis, D.E. Cintra, D.M. Tsukumo, G. Anhe, M.E. Amaral, H.K. Takahashi, R. Curi, H.C. Oliveira, J.B. Carvalheira, S. Bordin, M.J. Saad, L.A. Velloso, Saturated fatty acids produce an inflammatory response predominantly through the activation of TLR4 signaling in hypothalamus: implications for the pathogenesis of obesity, J. Neurosci. 29 (2009) 359–370.
[5] L. Ozcan, A.S. Ergin, A. Lu, J. Chung, S. Sarkar, D. Nie, M.G. Myers Jr., U. Ozcan, Endoplasmic reticulum stress plays a central role in development of leptin resistance, Cell Metab. 9 (2009) 35–51.
[6] J.P. Thaler, C.X. Yi, E.A. Schur, S.J. Guyenet, B.H. Hwang, M.O. Dietrich, X. Zhao, D.A. Sarruf, V. Izgur, K.R. Maravilla, H.T. Nguyen, J.D. Fischer, M.E. Matsen, B.E. Wisse, G.J. Morton, T.L. Horvath, D.G. Baskin, M.H. Tschop, M.W. Schwartz, Obesity is associated with hypothalamic injury in rodents and humans, J. Clin. Invest. 122 (2012) 153–162.
[7] X. Zhang, G. Zhang, H. Zhang, M. Karin, H. Bai, D. Cai, Hypothalamic IKKbeta/NF-kappaB and ER stress link overnutrition to energy imbalance and obesity, Cell 135 (2008) 61–73.
[8] J. Morari, G.F. Anhe, L.F. Nascimento, R.F. de Moura, D. Razolli, C. Solon, D. Guadagnini, G. Souza, A.H. Mattos, N. Tobar, C.D. Ramos, V.D. Pascoal, M.J. Saad, I. Lopes-Cendes, J.C. Moraes, L.A. Velloso, Fractalkine (CX3CL1) is involved in the early activation of hypothalamic inflammation in experimental obesity, Diabetes 63 (2014) 3770–3784.
[9] M. Valdearcos, J.D. Douglass, M.M. Robblee, M.D. Dorfman, D.R. Stifler, M.L. Bennett, I. Gerritse, R. Fasnacht, B.A. Barres, J.P. Thaler, S.K. Koliwad, Microglial inflammatory signaling orchestrates the hypothalamic immune response to dietary excess and mediates obesity susceptibility, Cell Metab. 26 (2017) 185–197 (e183).

[10] M. Valdearcos, M.M. Robblee, D.I. Benjamin, D.K. Nomura, A.W. Xu, S.K. Koliwad, Microglia dictate the impact of saturated fat consumption on hypothalamic inflammation and neuronal function, Cell Rep. 9 (2014) 2124–2138.
[11] C. Garcia-Caceres, E. Fuente-Martin, J. Argente, J.A. Chowen, Emerging role of glial cells in the control of body weight, Mol. Metab. 1 (2012) 37–46.
[12] E. Fuente-Martin, C. Garcia-Caceres, M. Granado, M.L. de Ceballos, M.A. Sanchez-Garrido, B. Sarman, Z.W. Liu, M.O. Dietrich, M. Tena-Sempere, P. Argente-Arizon, F. Diaz, J. Argente, T.L. Horvath, J.A. Chowen, Leptin regulates glutamate and glucose transporters in hypothalamic astrocytes, J. Clin. Invest. 122 (2012) 3900–3913.
[13] J.Y. Kwak, M. Mamura, J. Barlic-Dicen, E. Grage-Griebenow, Pathophysiological roles of cytokine-chemokine immune network, J Immunol Res 2014 (2014) 615130.
[14] V. Salvi, F. Sozio, S. Sozzani, A. Del Prete, Role of atypical chemokine receptors in microglial activation and polarization, Front. Aging Neurosci. 9 (2017) 148.
[15] F. Bachelerie, G.J. Graham, M. Locati, A. Mantovani, P.M. Murphy, R. Nibbs, A. Rot, S. Sozzani, M. Thelen, New nomenclature for atypical chemokine receptors, Nat. Immunol. 15 (2014) 207–208.
[16] C.A. Hansell, L.M. MacLellan, R.S. Oldham, J. Doonan, K.J. Chapple, E.J. Anderson, C. Linington, I.B. McInnes, R.J. Nibbs, C.S. Goodyear, The atypical chemokine receptor ACKR2 suppresses Th17 responses to protein autoantigens, Immunol. Cell Biol. 93 (2015) 167–176.
[17] L. Liu, G.J. Graham, A. Damodaran, T. Hu, S.A. Lira, M. Sasse, C. Canasto-Chibuque, D.N. Cook, R.M. Ransohoff, Cutting edge: the silent chemokine receptor D6 is required for generating T cell responses that mediate experimental autoimmune encephalomyelitis, J. Immunol. 177 (2006) 17–21.
[18] X. Fang, K. Ge, C. Song, Y. Ge, J. Zhang, Effects of n-3PUFAs on autophagy and inflammation of hypothalamus and body weight in mice, Biochem. Biophys. Res. Commun. 501 (2018) 927–932.
[19] S.Y. Chou, R. Ajoy, C.A. Changou, Y.T. Hsieh, Y.K. Wang, B. Hoffer, CCL5/RANTES contributes to hypothalamic insulin signaling for systemic insulin responsiveness through CCR5, Sci. Rep. 6 (2016) 37659.
[20] D.P. Zhao, C.L. Yang, X. Zhou, J.A. Ding, G.N. Jiang, Association between CLPTM1L polymorphisms (rs402710 and rs401681) and lung cancer susceptibility: evidence from 27 case-control studies, Mol. Gen. Genomics. 289 (2014) 1001–1012.
[21] E.P. Araujo, C.T. de Souza, L.A. Velloso, Atypical transforming growth factor-beta signaling in the hypothalamus is linked to diabetes, Nat. Med. 20 (2014) 985–987.
[22] J. Yan, H. Zhang, Y. Yin, J. Li, Y. Tang, S. Purkayastha, L. Li, D. Cai, Obesity- and aging-induced excess of central transforming growth factor-beta potentiates diabetic development via an RNA stress response, Nat. Med. 20 (2014) 1001–1008.
[23] A.S. Garfield, B.P. Shah, C.R. Burgess, M.M. Li, C. Li, J.S. Steger, J.C. Madara, J.N. Campbell, D. Kroeger, T.E. Scammell, B.A. Tannous, M.G. Myers Jr., M.L. Andermann, M.J. Krashes, B.B. Lowell, Dynamic GABAergic afferent modulation of AgRP neurons, Nat. Neurosci. 19 (2016) 1628–1635.
[24] M. Milanski, A.P. Arruda, A. Coope, L.M. Ignacio-Souza, C.E. Nunez, E.A. Roman, T. Romanatto, L.B. Pascoal, A.M. Caricilli, M.A. Torsoni, P.O. Prada, M.J. Saad, L.A. Velloso, Inhibition of hypothalamic inflammation reverses diet-induced insulin resistance in the liver, Diabetes 61 (2012) 1455–1462.
[25] P.A. Andreux, E.G. Williams, H. Koutnikova, R.H. Houtkooper, M.F. Champy, H. Henry, K. Schoonjans, R.W. Williams, J. Auwerx, Systems genetics of metabolism: the use of the BXD murine reference panel for multiscalar integration of traits, Cell 150 (2012) 1287–1299.
[26] G.F. Souza, C. Solon, L.F. Nascimento, J.C. De-Lima-Junior, G. Nogueira, R. Moura, G.Z. Rocha, M. Fioravante, V. Bobbo, J. Morari, D. Razolli, E.P. Araujo, L.A. Velloso, Defective regulation of POMC precedes hypothalamic inflammation in diet-induced obesity, Sci. Rep. 6 (2016) 29290.
[27] R.A. Ribeiro, T.M. Batista, F.M. Coelho, A.C. Boschero, G.S. Lopes, E.M. Carneiro, Decreased beta-cell insulin secretory function in aged rats due to impaired Ca(2+) handling, Exp. Physiol. 97 (2012) 1065–1073.